1293

Image registration with structuralized Mutual Information: application to CEST

Bian Li[1], Huajun She[1], Shu Zhang[1], Jochen Keupp[2], Ivan Dimitrov[3], Albert Montillo[1], Ananth Madhuranthakam[1], Robert Lenkinski[1], and Elena Vinogradov[1]

[1]Department of Radiology, Advanced Imaging Research Center, UT Southwestern Medical Center, Dallas, TX, United States, [2]Philips Research, Hamburg, Germany, [3]Philips Healthcare, Gainesville, FL, United States

Synopsis

In image registration, mutual information (MI) has proved to be an effective similarity measure and is widely used for medical image registration. However, the MI algorithm does not consider spatial dependencies of voxels and introduces significant errors when registering images with large intensity changes, like in Z-spectral images of CEST-MRI. This abstract shows that by the incorporation of structural information the SMI algorithm demonstrates robust performance registering Z-spectral images with large and complex intensity variations.

Purpose

Image registration plays an important role to effectively integrate data information. In CEST-MR imaging, inconsistent appearance of the same observables in different acquisitions makes the registration process challenging. Mutual information (MI) based registration was first independently proposed by Collignon [1] and Viola [2] in the mid-90s and has been successfully used for a large variety of combinations including MR, CT, PET, and SPECT [3]. However MI based registration is prone to fail in processing CEST images mainly because it only utilizes statistic information on voxel intensities. Here a structuralized MI (SMI) based algorithm is proposed to solve the problem. Tests from synthetic images and in-vivo studies show that compared with MI, the SMI algorithm provides robust results when registering Z-spectral images in CEST-MRI with large spatial intensity variations.

Methods

The new similarity measure of SMI incorporates the structural information of images and is defined as:

$$SMI = (NMI(A,B) + C_1)^{1-C_s} \cdot (2 \cdot cov(A,B) \big/ ((\sigma_A^2 + \sigma_B^2) + C_2))^{C_s}.$$

Here A and B are the reference and target images. NMI means normalized mutual information. σ_A^2, σ_B^2 and $cov(A,B)$ stand for variance and covariance of A and B respectively [4]. C_s indicates the degree of structural sensitivity with a default value of 0.5. C_1 and C_2 are used to increase the stability of the algorithm. SMI was tested and compared with MI by using synthetic images and Z-spectral kidney images. As shown in Fig. 1, a synthetic reference image was created using a pure white square block (14×14 pixels) at the center of a pure black background (40 × 40 pixels). A target image (30 × 30 pixels) was produced by symmetrically cropping four borders of the reference. As shown in Fig. 1(b), to simulate practical Z-spectral images, the target was degraded by decreasing the contrast and varying the intensity distribution so that its lower left area appeared slightly darker than the upper right area. Then the target image was shifted voxel-wise over the reference horizontally and vertically. MI and SMI similarities in the superimposed areas were calculated for each translation. The position of maximum value of MI or SMI calculation corresponds to the registered location found by each algorithm and the small target is supposed to register to the center of reference. The kidney CEST imaging experiments were performed on a Philips 3T Ingenia system with a 32 channel torso array coil (Philips, The Netherlands). Timed-breathing approach [5] was used to synchronize breathing motion with saturation-acquisition cycles. The following parameters were used: FOV = 209 × 362 mm, matrix = 104 × 179, voxel size = 2.0 × 2.0 mm, slice thickness = 5 mm, 2D single shot TSE, TR/TE = 6000/4.9 ms, coronal orientation and second-order PB-volume shimming. The saturation RF pulse train consisted of 40 SincGauss pulses, each 50ms duration, swept between ±550 Hz in steps of 78.6 Hz (total of 16 Z-spectral images, including reference). B0 inhomogeneity was corrected by WASSR technique [6]. Motion correction with MI or

Figures

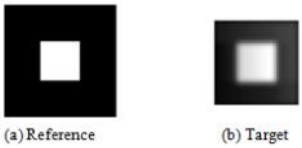

Fig.1 Synthetic images

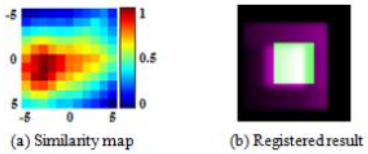

Fig. 2 MI registration

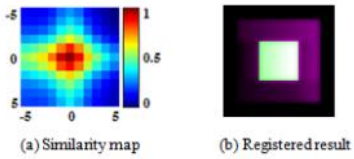

Fig. 3 SMI registration

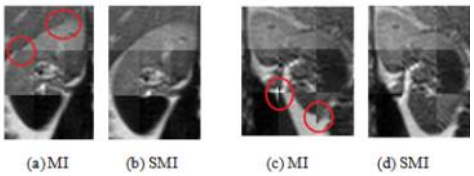

Fig. 4 Composite images: (a-b) right kidney, (c-d) left kidney; (a,c) MI registration, (b,d) SMI registration

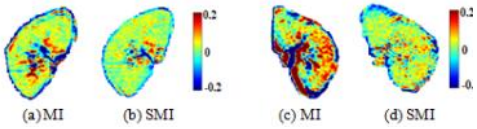

Fig. 5 MTRasym (2ppm) maps: (a-b) right kidney, (c-d) left kidney; (a,c) MI registration, (b,d) SMI registration

SMI was applied to TSE and WASSR data. CEST maps were calculated based on the Magnetization Transfer Asymmetry (MTRasym) [7] at 2ppm using motion corrected data.

Results and Discussion

In Fig.2, similarity value maps (11 × 11) were produced for MI in Fig. 2(a) and SMI measure in Fig. 2(b) and the values were normalized (0 to 1 scale).. The SMI measure correctly found the location of maximum value and the target was correctly registered with SMI. However, the MI measure resulted in misalignments (row offset = 1 pixel, column offset = -3 pixels). The example shows that intensity variations significantly lowered the reliability of MI, while SMI is more robust due to additional consideration of structural information. To review the kidney data after registration, nine equally-sized blocks from different parts of nine images were put together as a composite, as shown in Fig 4. Areas in the red circles in Fig. 4 (a) and (c) (MI algorithm) demonstrate obvious misalignments. MTRasym (2ppm) maps are shown in Fig. 5. After SMI registration (Fig.5 (b) and (d)), the MTRasym map became more homogenous and large intensity variations around papillas and borders, as visible in MI registration (Fig. 5(a) and (c)), disappeared.

Conclusion

The MI algorithm introduced significant errors when registering Z-spectral images for CEST-MRI, especially for regions with large intensity variations. By incorporation of structural information the SMI algorithm demonstrates robust performance registering images with large and complex intensity variations. The algorithm can be applied to other MRI experiments (e.g. DCE, ASL) and imaging modalities.

Acknowledgements

No acknowledgement found.

References

[1] Collignon, A., et al. Automated multi-modality image registration based on information theory. In Information processing in medical imaging, 1995. 3(6): p. 263-274.

[2] Viola, P. and A. Chao, Multiple sensor image alignment by maximization of mutual information. Massachusetts Institute of Technology and ALPHATECH, Inc, 1995.

[3] Maes, F., D. Vandermeulen, and P. Suetens, Medical image registration using mutual information. Proceedings of the IEEE, 2003. 91(10): p. 1699-1722.

[4] Wang, Z., et al., Image quality assessment: from error visibility to structural similarity. IEEE transactions on image processing, 2004. 13(4): p. 600-612.[5] Robson, P.M., et al., Strategies for Reducing Respiratory Motion Artifacts in Renal Perfusion Imaging With Arterial Spin Labeling. Magnetic Resonance in Medicine, 2009. 61(6): p. 1374-1387.

[6] Kim, M., et al., Water saturation shift referencing (WASSR) for chemical exchange saturation transfer (CEST) experiments. Magnetic resonance in medicine, 2009. 61(6): p. 1441-1450.

[7] Vinogradov, E., A.D. Sherry, and R.E. Lenkinski, CEST: from basic principles to applications, challenges and opportunities. J Magn Reson, 2013. 229: p. 155-172.